J. Phys. B: At. Mol. Opt. Phys. **23** (1990) 2405S-2424S. Printed in the UK

Low-energy electron–CH_4 collisions using exact exchange plus parameter-free polarisation potential

P McNaughten†, D G Thompson† and Ashok Jain‡

† Department of Applied Mathematics and Theoretical Physics, The Queen's University, Belfast BT7 1NN, UK

‡ Department of Physics, Box 981, Florida A&M University, Tallahassee, FL 32307, USA

Received 22 January 1990, in final form 20 February 1990

Abstract. Results are reported for the rotationally elastic, inelastic and summed cross sections (differential, integral, momentum transfer and energy loss) for electron-CH_4 scattering in the 0.1-20 eV energy region. Electron exchange is treated exactly and distortion effects are included using the parameter-free model polarisation potential. Agreement with available experimental measurements is good. The present results are also compared with other theoretical treatments. We also report the value of scattering length from the present model.

1. Introduction

This paper is a continuation of our recent work on electron-CH_4 slow ($E \leqslant 20$ eV) collisions (McNaughton and Thompson 1988, hereafter referred to as I), where for the first time the deficiencies of the popular free electron gas exchange (FEGE) model for electron exchange were clearly exhibited. A proper test of an approximate parameter-free and local polarisation potential proposed in the earlier work of Jain and Thompson (1982) was also made. Comparisons with experimental results for integral (rotationally summed) cross sections were encouraging, particularly at low energies, and supported the suggestion that the model polarisation potential is a reasonable representation of *molecular distortion*. In a more recent communication (Jain *et al* 1989), we tested several parameter-free models for the polarisation effects in the exact exchange calculation of I. We were led to believe that the exact exchange and a local and real polarisation approximation could also be used profitably for calculating nuclear inelastic processes.

The first part of the present work is to test this supposition by calculating rotational excitation cross sections under the adiabatic nuclei rotation (ANR) approximation using the same model approach as in I. We present results in section 3.1 which agree closely with recent experimental data of Müller *et al* (1985). This contrasts with the earlier work of Jain and Thompson (1983), using FEGE (Hara 1967 version) plus model polarisation (Jain and Thompson 1982, as mentioned above) interactions, which differs considerably from experiment and other recent theoretical work. In the second part of the paper, we have taken the opportunity to present full results for rotationally summed cross sections (differential, integral, momentum transfer and energy loss) at 0.1-20 eV impact energies in the same approximation.

We are particularly interested in comparing our results with other calculations in which the exchange effect is included exactly. One of these (Yuan 1988) is a spherical approximation (Jain 1983, 1986a) and thus is only a first approximation to the present

0953-4075/90/132405S+20$03.50

work; also it leads to pure elastic cross sections only. The other set of calculations began with Lima *et al* (1985) who reported the first results on the e-CH_4 system treating exchange effects exactly in a Schwinger multichannel (SMC) variational technique for scattering energies between 3 and 20 eV. Since this theory did not include polarisation effects, the comparison of their differential, total and momentum transfer cross sections with experiment is necessarily incomplete. More recently the same group (Lima *et al* 1989, Brescansin *et al* 1989) has included polarisation effects (we denote this approximation by SMP) for 3 to 20 eV impact energies. They have also calculated results for total and differential cross sections for the rotational excitation process in their energy range (Brescansin *et al* 1989). Lima *et al* (1989) have also reported their SMP results for the total cross section in the Ramsauer-Townsend (RT) minimum region (below 1 eV).

While not using exact exchange, there are two other interesting calculations for rotational excitation. Gianturco *et al* (1987) used the asymptotically adjusted version of the FEGE approach with a correlation polarisation potential also based upon the free electron gas model. Abusalbi *et al* (1983, 1987), in contrast to most investigations, formulated the problem using the laboratory coordinate frame rather than the molecular frame; the exchange potential was calculated in a semiclassical method and an approximate polarisation potential was also included. The results of Abusalbi *et al* are only for 10 eV, but they are in quite good agreement with experiment (Müller *et al* 1985).

The general theoretical and experimental situation for the e-CH_4 system before 1986 has been summarised in a review by Gianturco and Jain (1986). As well as the work described above, there have been several recent calculations using model approaches to both the exchange and polarisation effects, with varying degrees of success (Gianturco *et al* 1987, Gianturco and Scialla 1987, Bloor and Sherrod 1986, Jain 1986a, b). It is worth mentioning here that the differential cross sections (DCS) at very low energies (below 1 eV) are extremely sensitive to the approximations involved in a theoretical model. Unfortunately, there are no other theoretical DCS available, in which exchange is treated exactly along with polarisation effects, to compare with the present results.

The e-CH_4 system is a popular one for experimentalists. There are recent measurements on the total (σ_t) cross section due to Dababneh *et al* (1988) (1-500 eV), Lohmann and Buckman (1986) (0.1-20 eV), Ferch *et al* (1985) (0.085-12 eV), and Jones (1985) (1.3-50 eV) (for earlier references see the review by Gianturco and Jain (1986)). Swarm type experimental studies, providing data for the momentum transfer cross section (σ_m), have been performed by Haddad (1985) (0.01-10 eV) and Ohmori *et al* (1986) (0.05-50 eV). The low-energy DCS for the e-CH_4 system have recently been measured by several groups and the results agree reasonably well with each other: Shyn and Cravens (1989) (5-50 eV, 12°-156°); Sohn *et al* (1986) (0.2-5 eV, 15°-138°); Curry *et al* (1985) (7.5-20 eV, 32°-142°); Sohn *et al* 1983 (0.1-1.8 eV, 35°-105°); Tanaka *et al* (1982) (3-20 eV, 30°-140°); Rohr (1980) (0.1-10 eV, 20°-120°). This list does not include recent measurements on the e-CH_4 system at energies above 20 eV. For rotationally inelastic DCS the first measurements were made by Tanaka (1979) but there have been more recent and extensive results by Müller *et al* (1985) at 0.5, 5, 7.5 and 10 eV from 15° to 130°.

In section 2, we describe briefly the exchange plus polarisation approximation and the cross section formulae. In section 3, we present our results for rotational excitation cross sections, rotationally summed cross sections and energy-loss cross sections. Finally in section 4 we make some concluding remarks.

2. Theoretical set-up of the scattering problem

2.1. Full exchange plus polarisation model

At the static-exchange level (Lane 1980), the Schrödinger equation for the continuum electron function $F(\boldsymbol{r})$ in the body-fixed (BF) coordinate system can be written as,

$$[-\tfrac{1}{2}\nabla_r^2 + V_s(\boldsymbol{r}) - \tfrac{1}{2}k^2]F(\boldsymbol{r}) = \sum_\alpha \int \phi_\alpha^*(\boldsymbol{r}')|\boldsymbol{r}-\boldsymbol{r}'|^{-1}F(\boldsymbol{r}')\,\mathrm{d}\boldsymbol{r}'\phi_\alpha(\boldsymbol{r}) \tag{1}$$

where k is the incident electron wavevector and the static potential V_s is given by,

$$V_s(\boldsymbol{r}) = \int |\Phi_0|^2 \left(\sum_{j=1}^{N} |\boldsymbol{r}-\boldsymbol{r}_j|^{-1}\,\mathrm{d}\boldsymbol{r}_1\,\mathrm{d}\boldsymbol{r}_2 \ldots \mathrm{d}\boldsymbol{r}_N \right) - \sum_{i=1}^{M} Z_i|\boldsymbol{r}-\boldsymbol{R}_i|^{-1}. \tag{2}$$

Here Φ_0 is the target ground-state wavefunction given as a single Slater determinant of one-electron N spin orbitals $\phi_i(\boldsymbol{r})$ and M is the number of nuclei in the molecule.

In the static-exchange approximation (1), not all the short-range correlation is included and long-range polarisation of the target charge cloud is totally neglected. It is well known that these effects (particularly the long-range polarisation) must be included for a proper description of low-energy electron scattering. In the present work, we have allowed for charge distortion effects approximately by introducing a local and real polarisation potential $V_{\mathrm{pol}}(\boldsymbol{r})$ in (1). The values of V_{pol} at all $\boldsymbol{r}$ points were checked carefully. In brief, V_{pol} is parameter-free and calculated by the method of Pople and Schofield (1957) (PS) and the non-penetration criterion of Temkin (1957). In the PS method, the second-order energy of the target is determined from the first-order target wavefunction Φ_1 which is expanded in terms of Φ_0 and the expansion coefficients are evaluated variationally. The polarisibility (α_0) of the molecule determined from the PS method is within 20% of the correct value; we thus normalise the PS polarisation potential to yield the correct asymptotic behaviour of V_{pol} (see Jain and Thompson 1982).

Finally, after projecting the integro-differential equation (1) on to the symmetry-adapted angular basis functions of $F(\boldsymbol{r})$, we obtain a set of coupled integro-differential equations which can be written in a convenient matrix form, $\mathbf{LF} = \mathbf{WF}$, where $\mathbf{WF}$ is the exchange term. The iterative scheme is $\mathbf{LF}^i = \mathbf{WF}^{i-1}$, where $i = 0, 1, \ldots$. In order to start the solution, we chose $\mathbf{F}^0$ to be the solutions obtained from the asymptotically adjusted FEGE potential (Salvini and Thompson 1981). The equation (1) is solved for each symmetry (A_1, A_2, E, T_1 and T_2) and energy separately. The convergence with respect to number of iterations was tested for each state and also at the lower and the upper ends of the present energy region. We faced no convergence problems with or without polarisation effects. For the present CH_4 case, the other convergence parameters (the size of $\mathbf{K}$ matrix, expansion of potential terms and number of terms in the expansion of bound orbitals) were checked carefully and these details are exactly the same as described earlier (see Gianturco and Thompson 1976a, b, 1980, Jain and Thompson 1982, 1983, McNaughten and Thompson 1988).

In the following discussion, we will denote our full exchange plus polarisation calculation by the ESEP model while the ESE notation will represent the same results without any polarisation effects.

2.2. Cross section formulae

For full details we refer to our earlier paper (Jain and Thompson 1983) and the review article (Gianturco and Jain 1986). In the following, we provide only a summary of

various cross section formulae. We are concerned here with rotationally elastic, inelastic and summed channels for differential, integral, momentum transfer and energy-loss cross sections. As mentioned above, we solve our scattering problem in the fixed-nuclei approximation under the body-fixed (BF) frame of reference. In order to obtain physical parameters, we transform the BF scattering amplitude $f(\hat{\boldsymbol{k}}\cdot\hat{\boldsymbol{r}})$($\hat{\boldsymbol{k}}$ and $\hat{\boldsymbol{r}}$ are respectively the initial and final directions of the projectile) into the space-fixed (SF) amplitude $f(\hat{\boldsymbol{k}}\cdot\hat{\boldsymbol{r}}';\alpha\beta\gamma)$ (where $\hat{\boldsymbol{r}}'$ now refers the direction of scattered electron with respect to SF coordinate system and $(\alpha\beta\gamma)$ are the three Euler angles) by making use of rotation matrices. Even at the lower bound of the present energy region, the collision time is much less than the molecular rotational time period. Consequently, the ANR approximation is valid and the scattering amplitude for a particular rotational transition $JKM \to J'K'M'$ is written as (Chase 1957),

$$f(JKM \to J'K'M') = \langle \psi_{JKM} | f(\hat{\boldsymbol{k}}\cdot\hat{\boldsymbol{r}}';\alpha\beta\gamma) | \psi_{J'K'M'} \rangle \tag{3}$$

where $|\psi_{JKM}\rangle$ are the rotational eigenfunctions of a spherical top which are given as,

$$\psi_{JKM}(\alpha\beta\gamma) = \left(\frac{2J+1}{8\pi^2}\right)^{1/2} D^{J*}_{KM}(\alpha\beta\gamma). \tag{4}$$

Here K and M are projections of J along the BF and SF frame principal axes respectively. The differential cross section for the $J \to J'$ transition is obtained by summing over all final magnetic substates $K'M'$ and averaging over all the initial substates KM, i.e.,

$$\frac{\mathrm{d}\sigma}{\mathrm{d}\Omega}(J \to J') = \frac{k'}{k}\frac{1}{(2J+1)^2}\sum_{MM'KK'} |f(JKM \to J'K'M')|^2 \tag{5}$$

where k' is the wavenumber of the scattered electron given by the relation

$$2k'^2 = 2k^2 + E_J - E_{J'}. \tag{6}$$

The energy of the Jth level is calculated from $E_J = BJ(J+1)$, where B is the rotational constant of the CH_4 molecule. The value of B is taken to be 6.511×10^{-4} eV. It is convenient to express the DCS in terms of Legendre polynomials,

$$\frac{\mathrm{d}\sigma}{\mathrm{d}\Omega}(J \to J') = \frac{k'}{k}\sum_L A_L(J \to J') P_L(\cos\theta). \tag{7}$$

Here θ is the scattering angle between the vectors $\hat{\boldsymbol{k}}$ and $\hat{\boldsymbol{r}}'$. The expansion A_L coefficients are found to be (Jain and Thompson 1983),

$$A_L(J \to J') = \frac{(2J'+1)(2L+1)(-1)^L}{4k^2(2J+1)}\sum_{ll'\bar{l}\bar{l}'}[(2l+1)(2l'+1)(2\bar{l}+1)(2\bar{l}'+1)]^{1/2}\,\mathrm{i}^{l-l'}(-\mathrm{i})^{\bar{l}-\bar{l}'}$$
$$\times \begin{pmatrix} \bar{l} & l & L \\ 0 & 0 & 0 \end{pmatrix}\begin{pmatrix} l' & \bar{l}' & L \\ 0 & 0 & 0 \end{pmatrix}\sum_{j=|J-J'|}^{J+J'}(-1)^j W(ll'\bar{l}\bar{l}';jL) M^{jm_j}_{ll'} M^{jm_j*}_{\bar{l}\bar{l}'} \tag{8}$$

where the **M** matrix is defined as

$$M^{jm_j}_{ll'} = \sum_{mm'hh'p\mu}(-1)^m \bar{b}^{p\mu}_{lhm}\begin{pmatrix} l & l' & j \\ m & m' & -m_j \end{pmatrix}\bar{b}^{p\mu}_{l'h'm'}\mathbf{T}^{p\mu}_{lh,l'h'}. \tag{9}$$

Here, as usual, the **T** matrix is defined in terms of the **S** matrix as $\mathbf{T} = (\mathbf{S} - \mathbf{1})$ where $\mathbf{S} = (\mathbf{1} + \mathrm{i}\mathbf{K})(\mathbf{1} - \mathrm{i}\mathbf{K})^{-1}$ is written in terms of the scattering **K** matrix for each symmetry

$(p\mu)$. In (8), $\begin{pmatrix} a & b & c \\ d & e & f \end{pmatrix}$ is a $3-j$ symbol, $W(abcd; ef)$ is the well known Racah coefficient and the $b^{p\mu}_{lhm}$ coefficients are expansion terms in the definition of symmetry-adapted basis functions in terms of real spherical harmonics (see Gianturco and Jain 1986). From equation (6), it is easy to find simple forms for the σ_t and σ_m cross sections in terms of A_L coefficients, namely

$$\sigma_t^{JJ'} = 4\pi A_0(J \to J') \qquad \sigma_m^{JJ'} = 4\pi[A_0(J \to J') - \tfrac{1}{3}A_1(J \to J')]. \tag{10}$$

It is easy to determine A_0 and A_1 coefficients for σ_t and σ_m rather than the full expansion (7) and (8) for the DCS. For example, the A_0 and A_1 are given by the following simpler expressions,

$$A_0 = \frac{1}{4k^2} g(JJ') \sum_{ll'm_j} (-1)^{l+l'} |M^{jm_j}_{ll'}|^2 \tag{11}$$

and

$$\begin{aligned} A_1 = \frac{3}{4k^2} g(JJ') \sum_{ll'jm_j} (-1)^{l+l'+j} [&\{(l+1)(l'+1)\}^{1/2} W(ll'l+1l'+1; j1) M^{jm_j}_{ll'} M^{jm_j^*}_{l+1l'+1} \\ &+ \{l(l'+1)\}^{1/2} W(ll'l-1l'+1; j1) M^{jm_j}_{ll'} M^{jm_j^*}_{l-1l'+1} \\ &+ \{(l+1)l'\}^{1/2} W(ll'l+1l'-1; j1) M^{jm_j}_{ll'} M^{jm_j^*}_{l+1l'-1} \\ &+ (ll')^{1/2} W(ll'l-1l'-1; j1) M^{jm_j}_{ll'} M^{jm_j^*}_{l-1l'-1}] \end{aligned} \tag{12}$$

where $g(JJ')$ represents the statistical $(2J'+1)/(2J+1)$ factor. The vibrationally elastic (rotationally summed) cross sections are obtained by summing over J' for $J=0$. The selection rule for the transition $J \to J'$ can easily be worked our from the asymptotic form of the static potential (2) which transforms as $^1A_1$ symmetry of the T_d point group. For any specified values of J and J', the angular momentum transfer j (equations (8)-(9)) takes the following values,

$$|J-J'| \leqslant j \leqslant J+J' \qquad |l-l'| \leqslant j \leqslant l+l'. \tag{13}$$

Since in the vibrationally elastic scattering case, the CH_4 does not have any dipole and quadrupole moments, the essential torque for rotational excitation is provided by the non-zero octupole and other higher order moments of the molecule. In the present case of CH_4, our value of the octupole moment, 3.46, is about 17% smaller than the experimental value of 4.22 (see Bose *et al* 1972) in atomic units. Finally, for $J=0$, the allowed values of J' are $0, 3, 4 \ldots$, i.e. $|J-J'| = 0, 3, 4, 6, \ldots$ and so on. The rotational energy-loss cross section for a particular initial state J is given by (Norcross 1982)

$$\frac{dS^J}{d\Omega} = \sum_{J'} \tfrac{1}{2}(k^2 - k'^2) \frac{d\sigma}{d\Omega}(J \to J'). \tag{14}$$

The corresponding integral of (12) over scattering angles will be represented by S^J, known as the stopping cross section corresponding to initial rotational state J. We will show our results for S^0 and S^1 and discuss a general theorem by Shimamura (1981) which states that the energy-loss and stopping (as well as DCS and σ_t) cross sections are, when summed over final rotational states, independent of the initial

rotational state of the molecule in a situation where the rotational motion of the molecule is small during the collision time.

3. Results and discussion

3.1. Rotational excitation

In figures 1-4, we show our rotational excitation DCS (from $J = 0$ to $J' = 0, 3, 4$) at 0.5, 5.0, 7.5 and 10 eV respectively at all scattering angles. The cross sections for the $0 \rightarrow 6$ excitation are too small to include in the present discussion. These are the energies where experimental data of Müller *et al* (1985) are available for comparison. Let us first discuss the low-energy 0.5 eV curves in figure 1. The pure elastic DCS (figure 1(*a*))

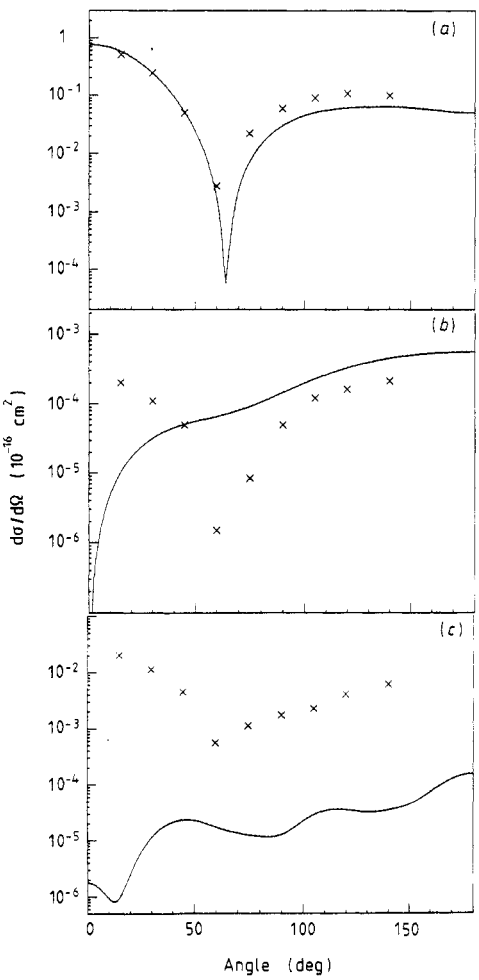

Figure 1. Rotationally elastic and inelastic DCS for the e-CH_4 collisions at 0.5 eV. Theory: full curve, present ESEP. Experiment: crosses, Müller *et al* (1986). The $0 \rightarrow 0$, $0 \rightarrow 3$ and $0 \rightarrow 4$ cases are shown respectively in (a), (b) and (c).

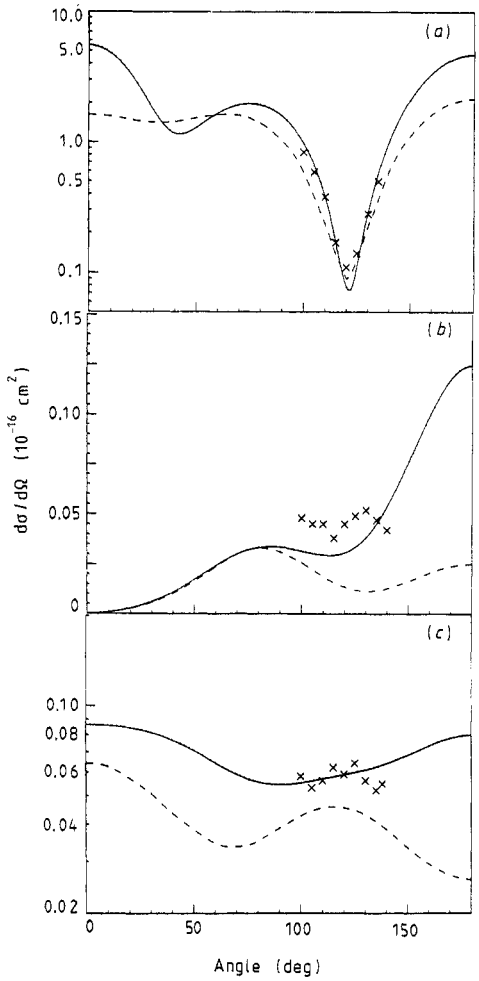

Figure 2. As figure 1, but for 5 eV. The broken curves are the SMP calculations of Brecansin *et al* (1989).

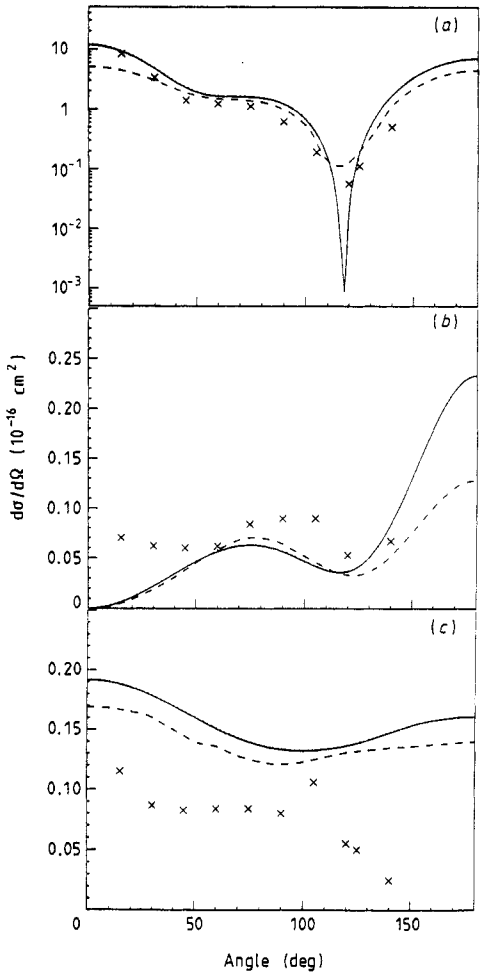

Figure 3. As figure 1, but for 7.5 eV.

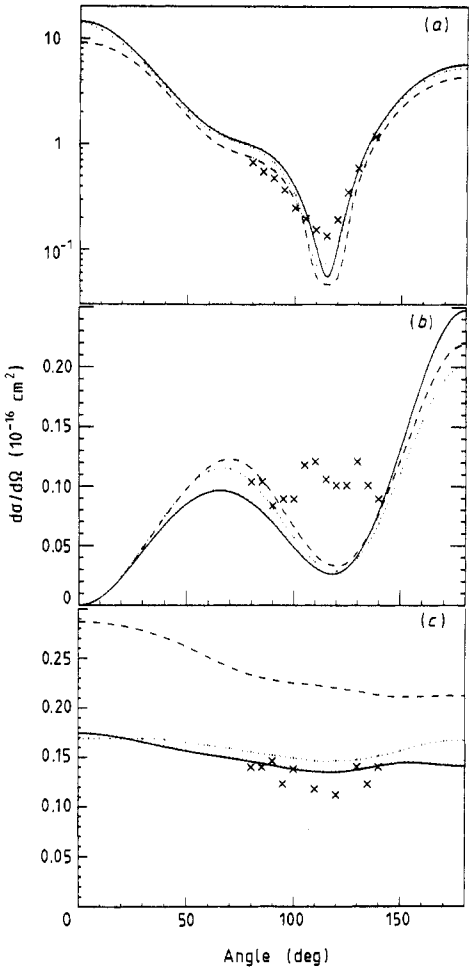

Figure 4. As figure 1 but for 10 eV. The dotted curves are the results of Abusalbi *et al* (1987).

of Müller *et al* (1985) reveal a minimum around 60° which is clearly reproduced by the present ESEP model without any fitting procedure; however, there is still a large discrepancy in the magnitude (about 50%) at large angle scattering. At this rather low energy, the DCS are supposed to be quite sensitive with respect to the level of approximations for exchange and polarisation effects. It means that our approximate parameter-free polarisation potential (Jain and Thompson 1982) is very successful when employed along with an exact-exchange treatment. This observation signifies the importance of an exact treatment of exchange at such low energies. The DCS on the $0 \rightarrow 3$ and $0 \rightarrow 4$ transitions are shown in parts (*b*) and (*c*) of figure 1. We notice a large discrepancy between theory and experiment for the $0 \rightarrow 4$ transition (figure 1(*c*)), while the $0 \rightarrow 3$ case does not show any reasonable agreement either. The experimental $0 \rightarrow 3$ points show a forward peaking feature with a minimum around 60°, while our theoretical DCS at 0.5 eV fall abruptly to zero in the forward direction and show no minimum at any angle. Some uncertainties in our inelastic DCS of figure 1 may be introduced due to the fact that there is some difference between our theoretical and the experimental

Table 1. Differential cross sections for the e-CH_4 rotationally elastic ($0\rightarrow0$), inelastic ($0\rightarrow3$ and $0\rightarrow4$) and summed processes. All numbers are in units of 10^{-16} cm^2. 1.78−6 means 1.78×10^{-6}.

	0.5 eV				1.0 eV				3.0 eV			
Angle (deg)	$0\rightarrow0$	$0\rightarrow3$	$0\rightarrow4$	Total	$0\rightarrow0$	$0\rightarrow3$	$0\rightarrow4$	Total	$0\rightarrow0$	$0\rightarrow3$	$0\rightarrow4$	Total
0	0.758	0.0	1.78−6	0.758	0.534	0.0	3.56−5	0.534	1.31	0.0	1.09−2	1.32
5	0.734	1.23−6	1.48−6	0.734	0.507	7.43−6	3.76−5	0.507	1.24	6.08−5	1.09−2	1.25
10	0.668	4.78−6	9.28−7	0.668	0.433	2.90−5	4.38−5	0.433	1.05	2.40−4	1.10−2	1.06
20	0.456	1.71−5	2.46−6	0.456	0.217	1.05−4	7.15−5	0.217	0.792	5.28−4	1.11−2	0.804
30	0.240	3.23−5	1.11−5	0.240	4.87−2	2.04−4	1.14−4	4.91−2	0.539	9.18−4	1.11−2	0.551
40	9.50−2	4.57−5	2.13−5	0.095	4.32−3	3.03−4	1.48−4	4.79−3	0.258	2.01−3	1.11−2	0.271
50	2.40−2	5.61−5	2.31−5	0.024	4.88−2	3.96−4	1.46−4	4.93−2	0.387	3.59−3	1.07−2	0.401
60	1.69−3	6.59−5	1.78−5	1.78−3	0.119	4.86−4	1.16−4	0.119	0.749	5.67−3	9.83−3	0.765
65	9.61−5	7.21−5	1.52−5	1.91−4	0.152	5.30−4	1.02−4	0.152	1.09	7.94−3	8.66−3	1.11
70	2.38−3	8.04−5	1.36−5	2.48−3	0.181	5.72−4	9.17−5	0.181	1.28	9.82−3	7.68−3	1.29
80	1.42−2	1.05−4	1.18−5	1.43−2	0.223	6.47−2	8.89−5	0.224	1.27	1.08−2	7.21−3	1.22
90	3.03−2	1.44−4	1.27−5	3.05−2	0.242	6.93−4	1.12−4	0.243	1.09	1.06−2	7.31−3	1.11
100	4.50−2	1.96−4	2.18−5	4.52−2	0.235	6.95−4	1.60−4	0.236	0.775	9.76−3	7.79−3	0.792
110	5.49−2	2.58−4	3.35−5	5.52−2	0.206	6.50−4	2.04−4	0.206	0.430	8.81−3	8.27−3	0.447
120	6.03−2	3.23−4	3.52−5	6.07−2	0.166	5.68−4	2.10−4	0.167	0.176	8.54−3	8.50−3	0.193
130	6.29−2	3.87−4	3.22−5	6.33−2	0.127	4.67−4	1.97−4	0.127	8.99−2	9.58−3	8.61−3	0.108
140	6.34−2	4.44−4	3.49−5	6.39−2	9.31−2	3.77−4	2.14−4	9.37−2	0.181	1.21−2	9.04−3	0.203
150	6.13−2	4.91−4	4.42−5	6.18−2	6.51−2	3.03−4	2.84−4	6.57−2	0.412	1.59−2	1.01−2	0.438
160	5.68−2	5.25−4	7.26−5	5.74−2	4.39−2	2.54−4	4.26−4	4.46−2	0.707	1.99−2	1.17−2	0.880
170	5.22−2	5.46−4	1.24−4	5.29−2	3.10−2	2.28−4	6.11−4	3.18−2	0.959	2.31−2	1.34−2	0.996
180	5.03−2	5.53−4	1.52−4	5.10−2	2.68−2	2.20−4	7.03−4	2.77−2	1.06	2.43−2	1.42−2	1.10

Table 1. (continued)

	5.0 eV				7.5 eV				10.0 eV			
Angle (deg)	0→0	0→3	0→4	Total	0→0	0→3	0→4	Total	0→0	0→3	0→4	Total
0	5.53	0.0	8.63−2	5.61	11.86	0.0	0.191	12.05	14.30	0.0	0.174	14.48
5	5.33	1.86−4	8.62−2	5.42	11.53	7.84−4	0.191	11.72	13.93	1.62−3	0.174	14.10
10	4.78	7.31−4	8.58−2	4.87	10.61	3.06−3	0.190	10.80	12.87	6.32−3	0.173	13.05
20	4.00	1.60−3	8.52−2	4.09	9.26	6.62−3	0.188	9.45	11.33	1.37−2	0.172	11.51
30	3.14	2.78−3	8.42−2	3.23	7.70	1.12−2	0.185	7.89	9.53	2.31−2	0.170	9.73
40	1.74	6.07−3	8.13−2	1.82	4.77	2.22−2	0.178	4.97	6.09	4.51−2	0.166	6.30
50	1.17	1.09−2	7.67−2	1.26	2.84	3.44−2	0.170	3.05	3.63	6.73−2	0.161	3.86
60	1.30	1.72−2	7.07−2	1.39	1.94	4.64−2	0.160	2.14	2.19	8.51−2	0.156	2.43
65	1.67	2.42−2	6.44−2	1.76	1.66	5.63−2	0.151	1.87	1.45	9.52−2	0.153	1.70
70	1.95	3.00−2	5.89−2	2.03	1.63	6.22−2	0.143	1.83	1.12	9.55−2	0.149	1.37
80	1.94	3.33−2	5.55−2	2.03	1.55	6.23−2	0.137	1.75	0.955	8.62−2	0.146	1.19
90	1.59	3.34−2	5.44−2	1.68	1.22	5.65−2	0.133	1.41	0.728	6.92−2	0.142	0.939
100	0.985	3.14−2	5.51−2	1.07	0.672	4.68−2	0.132	0.85	0.391	4.87−2	0.138	0.579
110	0.379	2.95−2	5.68−2	0.465	0.152	3.78−2	0.134	0.325	0.103	3.17−2	0.135	0.272
120	7.74−2	3.06−2	5.87−2	0.167	2.01−2	3.68−2	0.137	0.195	0.107	2.68−2	0.135	0.271
130	0.282	3.82−2	6.08−2	0.382	0.525	5.11−2	0.142	0.719	0.576	4.15−2	0.137	0.757
140	1.01	5.38−2	6.38−2	1.13	1.70	8.37−2	0.148	1.94	1.54	7.38−2	0.141	1.76
150	2.13	7.59−2	6.80−2	2.28	3.37	0.131	0.153	3.65	2.85	0.132	0.144	3.13
160	3.36	9.94−2	7.31−2	3.54	5.14	0.181	0.158	5.48	4.24	0.188	0.144	5.20
170	4.34	0.117	7.75−2	4.53	6.51	0.219	0.160	6.89	5.32	0.231	0.142	5.69
180	4.71	0.124	7.93−2	4.92	7.03	0.233	0.161	7.43	5.72	0.248	0.141	6.12

values of multipole moments of CH_4 (see section 2). At such low energies, these long-range forces (for example, octupole moment) may be very important. In addition, the accuracy of these weak rotational excitation cross section measurements is also not very clear; the measured cross sections are obtained indirectly by deconvolution of the vibrationally elastic peaks using an approximate analysis due to Shimamura (1983).

Figure 2 displays the $0 \rightarrow 0$, $0 \rightarrow 3$ and $0 \rightarrow 4$ DCS at 5 eV. Also shown in this figure are the SMP calculations of Brescansin *et al* (1989). Here, for all the three transitions, the present ESEP curves compare rather very well with the measurements relative to the SMP calculations of Brescansin *et al.* At this energy, the $0 \rightarrow 4$ agrees almost perfectly with the data of Müller *et al* (1985); however, this agreement may be fortuitous. It is rather interesting to note that the present ESEP results are very close with experimental points for the $0 \rightarrow 3$ excitation and almost identical for the higher $0 \rightarrow 4$ case. This trend of agreement between the present ESEP calculations and the experimental data of Müller *et al* continues at higher energies also; for example, at 7.5 eV (figure 3) and 10 eV (figure 4). The pure elastic $0 \rightarrow 0$ DCS (figures 3(a) and 4(a)) compare very well, while for the inelastic $0 \rightarrow 3$ case, our ESEP data are again better than the other theoretical prediction plotted there. At 10 eV, in figure 4, we have also plotted the results of Gianturco *et al* (1987) and Abusalbi *et al* (1987). Our ESEP DCS are closer to the calculations of Abusalbi *et al* rather than the SMP results of Brescansin *et al* (1989). The only exception of the ESEP agreement with experiment is the $0 \rightarrow 4$ transition at 7.5 eV (figure 3(c)); the ESEP numbers are higher by about a factor of two than the observations of Müller *et al* (1985). Also in figure 4(b), the experimental points are in disagreement with all the theoretical results plotted there at 10 eV for the $0 \rightarrow 3$ transition.

In table 1 we have provided our DCS at a few selected energies (0.5, 1.0, 3.0, 5.0, 7.5 and 10.0 eV). Above 10 eV, there are no experimental data on the rotational excitation channel. Since we found a large difference between our results and the data of Brescansin *et al* (1989) for the $0 \rightarrow 3$ and $0 \rightarrow 4$ transitions at and below 10 eV, it may be interesting to make this comparison at higher 15 and 20 eV energies where integral cross sections are of the order of a few atomic units. In figures 5 and 6 we show the two sets of theoretical (treating exchange exactly and polarisation approximately) inelastic cross sections ($0 \rightarrow 3$ and $0 \rightarrow 4$) at 15 and 20 eV respectively. We still see a significant discrepancy between two models which may be mainly due to the difference in the treatment of polarisation effects. It is, however, worth mentioning here that at 10 eV, ours as well as the calculations of Abusalbi *et al* (1983, 1987) are in fairly good agreement with measurements, while the Brescansin *et al* results agree poorly. In general the SMP results of Brescansin *et al* for the inelastic channels are higher than the present ESEP calculation (figures 5-6).

After looking at figures 1(b)-4(b) and figures 5(a) and 6(a) for the $0 \rightarrow 3$ transition, it is clear that theory predicts zero cross section in the forward direction; this seems to be in contrast with experimental observation, where, for example at 7.5 eV, the DCS seem to increase at lower angles. The vanishing of the theoretical $0 \rightarrow 3$ DCS in the forward direction may be due to the fact that in the calculation the initial ground state is assumed to be the $J = 0$; however, in the experimental situation, the target molecules are distributed over several J values at room temperature. Currently, we are in the process of investigating the effect of gas temperature on the rotationally inelastic DCS in the e-CH_4 collision (Jain and Thompson 1990). Another qualitative difference in the features of the measured and calculated DCS for this $0 \rightarrow 3$ case is the absence of

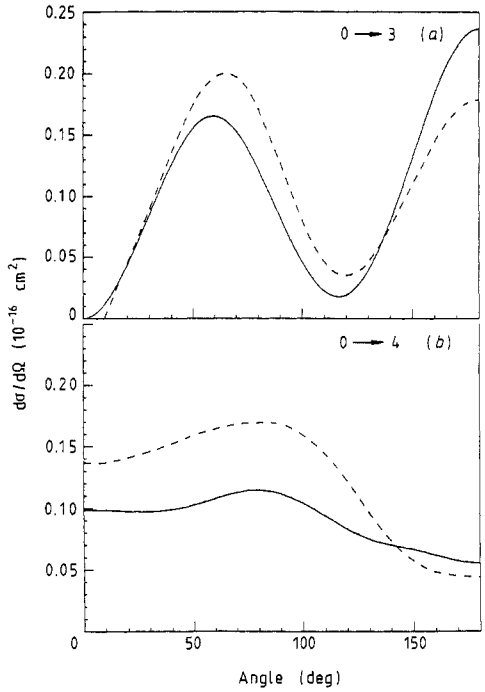

Figure 5. The $0 \rightarrow 3$ (a) and $0 \rightarrow 4$ (b) differential cross sections at 15 eV. Full curves, present ESEP results; broken curves, SMP calculations of Brescansin *et al* (1989).

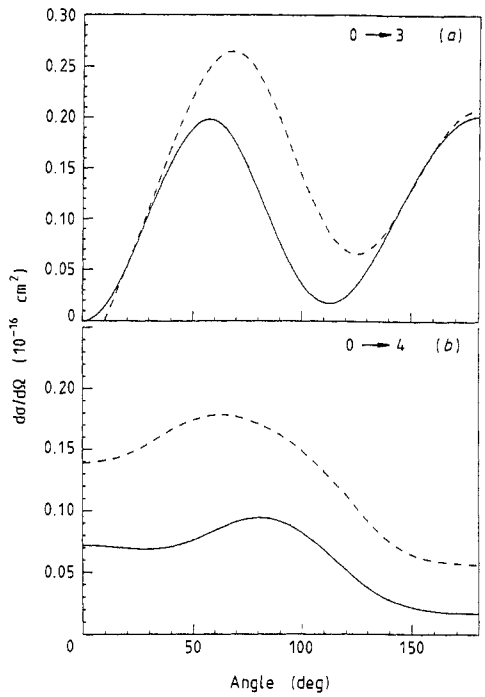

Figure 6. As figure 5, but for 20 eV.

a dip (observed in the experimental data around 60° at 0.5 eV) in the theoretical results (figure 1(b)). Also at 10 eV, all the theoretical DCS for the same $0 \rightarrow 3$ transition depict a minimum at 120°, while the experimental points seem to be flat. The minimum around 120° in the $0 \rightarrow 3$ transition exists even at higher energies at 15 (figure 5) and 20 (figure 6) eV energies. For the $0 \rightarrow 4$ excitation at 7.5 eV, the observed cross sections exhibit an abrupt drop beyond 100°, whereas the calculated values show a reverse trend. However, at higher energies ($E \geqslant 10$ eV), the $0 \rightarrow 4$ cross sections start decreasing beyond 100°.

Despite these discrepancies (see above) between theory and experiment (figures 1-4), and keeping in mind that the measurements are not direct, we can conclude that the ESEP model describes the low-energy rotational excitation DCS in CH_4 better than any other theoretical study available to date. We need more experimental studies on the rotational excitation of CH_4 molecules in order to access the creditibility of our theoretical model.

Next, we plot the integral quantities for the all the three cases ($\sigma^{00}_{t,m}$, $\sigma^{03}_{t,m}$, $\sigma^{04}_{t,m}$) in figures 7-9. These integral quantities are given in table 2 at all energies considered here. Also shown in these figures are the SMP calculations of Brescansin *et al* (1989). It is interesting to see that the two theories agree only qualitatively, while there is significant difference in their magnitudes. This is quite obvious since the two theoretical calculations give different behaviour of the DCS (see figures 1-6). At 10 eV, however, our results are closer to the calculations of Abusalbi *et al* (1987) than the SMP numbers of Brescansin *et al* (1989) for all cases. The data of figures 7-9 from 0.1 to 20 eV

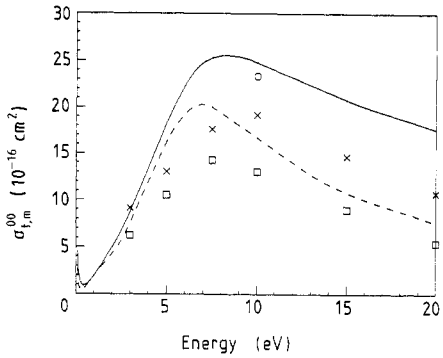

Figure 7. The integral (σ_t) (full curve) and momentum transfer (σ_m) (broken curve) rotationally elastic ($0 \rightarrow 0$) cross sections for e-CH_4 scattering in the present ESEP model. The SMP calculations of Brescansin *et al* (1989) are shown by squares (σ_t) and crosses (σ_m). The calculation of Abusalbi *et al* (1987) at 10 eV only is shown by a circle. For various notations, see the text.

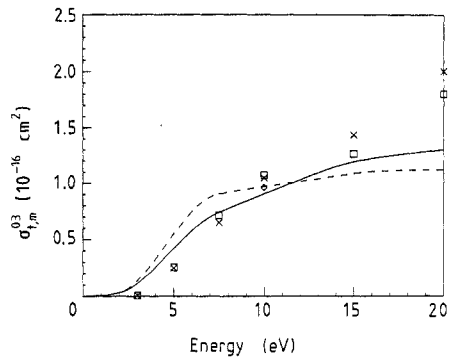

Figure 8. As figure 7, but for the $0 \rightarrow 3$ rotational transition.

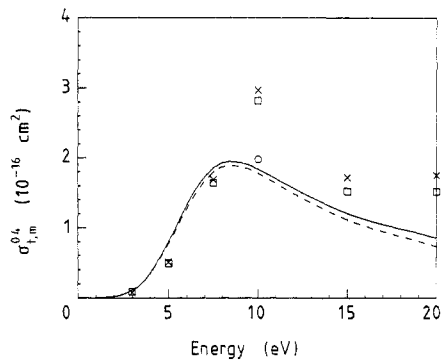

Figure 9. As figure 7, but for the $0 \rightarrow 4$ rotational excitation.

indicate that the 7-8 eV structure exists mainly in the elastic and the $0 \rightarrow 4$ cases, which is due to d-wave dominance in both the channels. The $0 \rightarrow 3$ channel also exhibits some little structure (figure 8) in its energy dependence. The $0 \rightarrow 0$ cross sections dominate the scattering event at all energies. This reflects the almost spherical nature of CH_4 molecule. In this respect our σ_t^{00} cross sections are very close to the calculations of Yuan (1988) who has included exchange effects exactly in an iterative approach (along with a different polarisation potential) but using a spherical model for the CH_4 target.

3.2. Rotationally summed cross sections

In the first paper of this work (I), we have already presented the ESEP σ_t cross sections in the whole energy region (0.1-20 eV) considered here. Here we concentrate mainly on the DCS and the σ_m quantities not reported in I. In I we have already demonstrated the success of the present ESEP calculation in reproducing quite accurately the RT structure (both position and the magnitude of the σ_t) and the broad hump feature around 7-8 eV. As mentioned earlier, the DCS present a rather stringent test of any

Table 2. Rotational excitation cross sections for the e-CH_4 system (10^{-16} cm^2) in the ESEP model. 6.57 − 5 means 6.57×10^{-5}.

	σ_t				σ_m			
Energy (eV)	0→0	0→3	0→4	Total	0→0	0→3	0→4	Total
0.1	4.46	6.57 − 5	3.26 − 5	4.46	2.68	1.04 − 3	3.95 − 5	2.68
0.2	1.95	3.91 − 4	7.22 − 5	1.95	6.37 − 1	6.12 − 4	8.87 − 5	6.38 − 1
0.3	1.143	9.79 − 3	1.20 − 4	1.144	2.76 − 1	1.50 − 3	1.52 − 4	2.78 − 1
0.4	0.91	1.73 − 3	1.97 − 4	0.91	3.76 − 1	2.57 − 3	2.54 − 4	3.79 − 1
0.5	0.91	2.52 − 3	3.20 − 4	0.91	6.11 − 1	3.63 − 3	4.15 − 4	6.15 − 1
0.6	1.02	3.30 − 3	4.91 − 4	1.025	8.81 − 1	4.53 − 3	6.37 − 4	8.86 − 1
0.8	1.41	4.70 − 3	1.07 − 3	1.42	1.41	5.71 − 3	1.36 − 3	1.417
1.0	1.90	6.14 − 3	2.09 − 3	1.91	1.89	6.44 − 3	2.57 − 3	1.90
2.0	4.94	3.26 − 2	2.28 − 2	4.99	4.24	3.37 − 2	2.42 − 2	4.30
3.0	8.73	0.115	0.112	8.96	7.55	0.139	0.111	7.80
4.0	13.35	0.252	0.355	13.96	11.92	0.322	0.344	12.58
5.0	18.29	0.420	0.799	19.51	16.34	0.548	0.772	17.66
6.0	22.36	0.578	1.329	24.27	19.31	0.747	1.283	21.35
7.5	25.28	0.738	1.856	27.88	20.02	0.901	1.795	22.73
10.0	24.81	0.903	1.840	27.58	16.75	0.968	1.778	19.53
15.0	20.83	1.189	1.20	23.28	10.81	1.086	1.114	13.10
20.0	17.60	1.297	0.850	19.85	7.575	1.119	0.729	9.56

theoretical model. In this energy range we have several sets of experimental data for comparison (see section 1). In a more recent communication (Jain *et al* 1989), we have shown that the present ESEP model with the Jain and Thompson (1982) polarisation model is better than the corresponding ESEP calculation using another parameter-free polarisation model based on the correlation energy (see O'Connel and Lane 1983, Gianturco *et al* 1987).

First, in figure 10, we have plotted our present ESEP total DCS at 0.2 eV along with the absolute measured quantities of Sohn *et al* (1986). The agreement between these

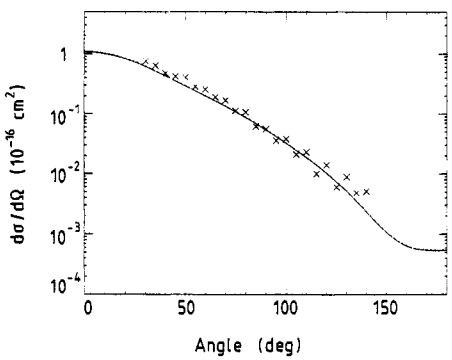

Figure 10. Rotationally summed (vibrationally elastic) differential cross sections for the e-CH_4 collisions at 0.2 eV. Present theory (ESEP) is shown by the full curve while the experimental data of Sohn *et al* (1986) are plotted by crosses.

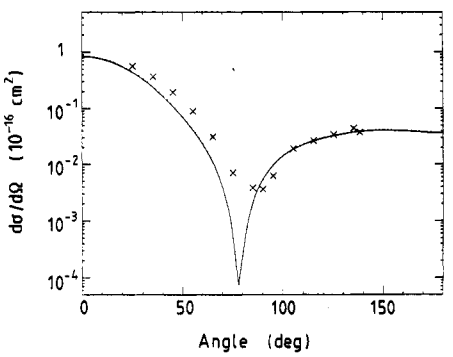

Figure 11. As figure 10, but for 0.4 eV.

ESEP and the observed angular functions is rather very good both in quality and quantity. In this low energy region no other exact-exchange plus polarisation type calculation is available for comparison. Our earlier results (Jain and Thompson 1983) with model free electron gas exchange approximation are not good at all below 1 eV (for this comparison see Jain *et al* 1989). The absence of a vibrational excitation process at 0.2 eV gives us more confidence about our present ESEP calculation. It should be realised here that at such a low energy the structure of the DCS in the whole energy region is decided jointly by exchange and the polarisation forces. That is why the same polarisation model (PS) behaves so differently with different levels of exchange approximation (Jain *et al* 1989). At such a low impact energy, the DCS are still not isotropic and change by three orders of magnitude by going from lower to higher angles.

As the energy is increased, for example at 0.4 eV in figure 11, the DCS are characterised by a minimum around 80°-90°, which is mainly due to the mixing of p wave (in the T_2 symmetry). Here at 0.4 eV, the ESEP and experimental DCS are in fairly qualitative agreement with each other. Note that this energy is very close to the position of the RT minimum where the cross sections are going to be very small and influenced significantly by the RT effect. We are tempted here to show another set of curves in figure 12 at 0.6 eV. At this energy also, we can see that the present ESEP model describes the rotationally averaged scattering process quite accurately. In all these figures (10-12), the inclusion of polarisation effects makes drastic changes in the shape of the DCS. In order to see the RT effect with respect to the differential scattering, we have plotted the same DCS in the RT energy region as a function of energy at few selected middle angles. Figure 13 clearly illustrates the RT effect around 0.4 eV in the angular distribution function.

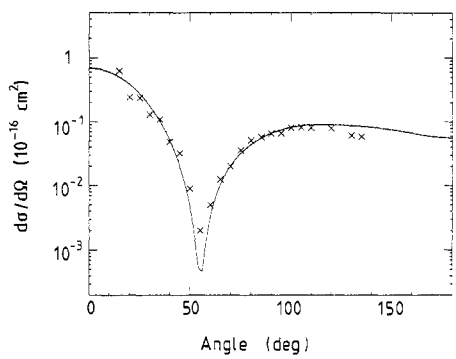

Figure 12. As figure 10, but for 0.6 eV.

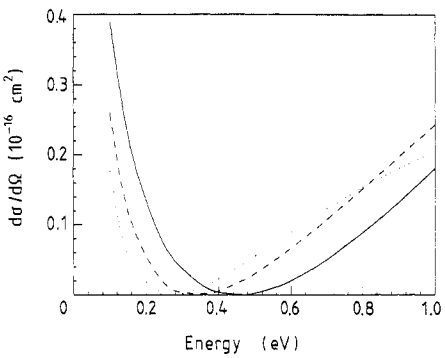

Figure 13. Differential cross sections for the e-CH_4 collisions as a function of energy at few scattering angles. Full curve, 70°; broken curve, 90°; dotted curve, 110°.

At and above 1 eV energy, the present ESEP theory maintains its success. At 1 eV (figure 14), we have also included earlier measurements of Rohr (1980). Unfortunately, even at 1 eV, no other theoretical results, including electron exchange exactly, are available for comparison. We now show our ESEP DCS at those higher energies (3, 5 and 7.5 eV) where *ab initio* SMP results of Brescansin *et al* (1989) are available. We have not shown any DCS at 10 eV, since at this relatively higher energy, even a simple spherical model (Jain 1986a) gives very good results. We can see from figures 14-17

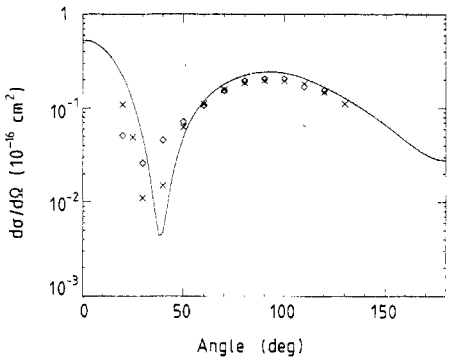

Figure 14. As figure 10, but for 1 eV. The squares are the measurements of Rohr (1980).

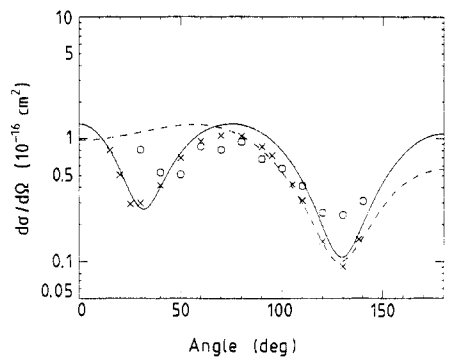

Figure 15. As figure 14 except that the extra data are from: theory, broken curve of Brescansin *et al* (1989); experiment, circles are from Tanaka *et al* (1982).

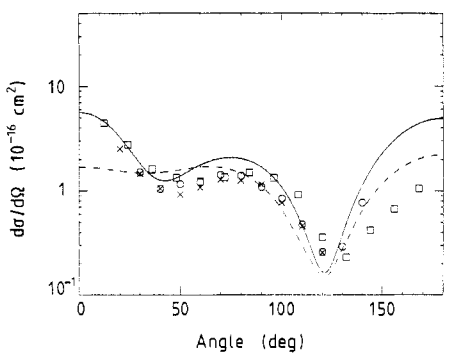

Figure 16. As figure 10 but for 5 eV. The new data (squares) are taken from the measurements of Shyn and Cravens (1989).

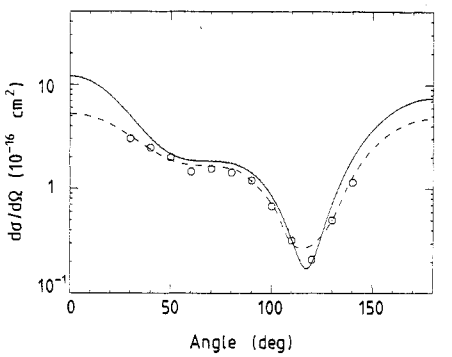

Figure 17. As figure 15, but for 7.5 eV.

that the present ESEP model is in good agreement with measured values and in most cases is much better than the other theoretical curves shown in these figures. In this energy region, several other experimental data are available (Tanaka *et al* 1982, Shyn and Cravens 1989) which are in reasonable agreement with each other. Our ESEP calculations reproduce all the salient features (except for some discrepancy in the backward direction) in the angular distribution function observed experimentally, while the SMP theory has considerable discrepancy in the forward direction with our ESEP as well as with the experimental results. For example, at 3 eV (figure 15), a small-angle dip around 30°, observed in the laboratory, is missing from the SMP curve.

Although the ESEP σ_t have already been discussed earlier (McNaughten and Thompson 1988) in the RT (0.1-1 eV) (see also Jain *et al* 1989) and broad feature (1-15 eV) energy regions, it is interesting to compare these results in the 1-15 eV region with more recent beam-transmission experimental data of Dababneh *et al* (1988). In figure 18, our ESEP σ_t results are plotted along with three recent measurements due to Ferch *et al* (1985), Lohmann and Buckmann (1986) and Dababneh *et al* (1988). Also shown in figure 18 are the theoretical OMSCE calculations of Gianturco and Scialla (1987) (using a modified version of the semiclassical-exchange approximation with

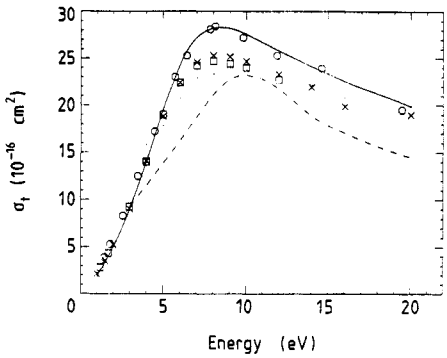

Figure 18. Total (σ_t) cross sections for the e-CH_4 collisions at 1-20 eV using the present ESEP model. Other theories: dotted curve, Gianturco and Scialla (1987); broken curve, Brescansin *et al* (1989). Experimental data: circles, Dababneh *et al* (1988); squares, Ferch *et al* (1985); crosses, Lohmann and Buckman (1985).

orthogonalisation technique) and a correlation polarisation potential (see O'Connel and Lane 1983 for the general theory). The SMP numbers of Brescansin *et al* (1989) are also included in figure 18. It is seen from figure 18 that the present ESEP results seem to follow the data of recent measurements of Dababneh *et al* (1988); this trend is followed at all energies considered in figure 18. Finally, our momentum transfer cross sections are shown in figure 19 along with the theoretical SMP values of Brescansin *et al* (1989) and the swarm data of Haddad (1985) and Ohmari *et al* (1986). In figure 19, we also show the experimental estimate of Tanaka *et al* (1982) from the integral of their measured DCS, which always involves some uncertainty due to the extrapolation procedure. Note that the position of the RT minimum in the σ_m occurs somewhat at lower energies than the corresponding position in the σ_t values. Our agreement of σ_m cross section is qualitative (particularly below 3 eV where swarm analysis is more accurate) with the swarm data and the measurements of Tanaka *et al* (1982). However, at the RT minimum, the experimental σ_m are about a factor of two higher than the present ESEP results (see figure 19(*a*)). On the other hand, in the broad hump region,

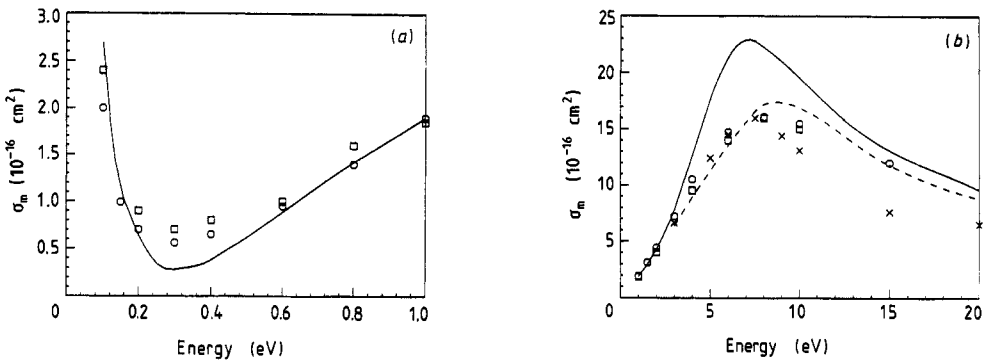

Figure 19. (*a*) σ_m cross sections for the e-CH_4 scattering at 0.1-1 eV in the present ESEP model (full curve). Experimental data: squares, Haddad (1985); circles Ohmari *et al* (1987). (*b*) As (*a*) but for the 1-20 eV energy region. The broken curve is the SMP calculation of Brescansin *et al* (1989) and the crosses are the experimental points of Tanaka *et al* (1982).

our ESEP σ_m cross sections are much higher (50%) than all other theoretical and experimental data.

3.3. Scattering length (a_0)

Finally, we extended our calculations towards the zero-energy limit (where only the s wave of the A_1 symmetry is important) in order to extract information on the scattering length, a_0, defined as,

$$\lim_{k\to 0} \cot \delta_0^{A_1}(k)) = -\frac{1}{a_0} \tag{15}$$

where $\delta_0^{A_1}(k)$ is the s wave phaseshift in the A_1 symmetry at energy k^2. Our zero-energy limit of the phaseshift was checked at several energies of 0.005, 0.001 and 0.0005 eV; the convergence of the a_0 value was good. In this very low energy limit, one has to be careful about the accuracy of the K matrix (its symmetric property) as well as the proper convergence with respect to the number of iterations: we needed about 25 iterations for the A_1 symmetry to ensure the desired accuracy. Recently, Ferch *et al* (1985) have estimated a_0 to be -2.475 au. Our earlier value (Jain 1986b) for a_0 is -3.41 au, which was obtained by a polarisation potential tuned to give the correct behaviour of the RT effect. The present ESEP value of a_0 is -2.9 au, which is within 15% of the observed value of Ferch *et al* (1985).

3.4. Energy-loss and stopping cross sections

It is quite easy to generate energy-loss (equation (14)) and stopping cross sections from the present rotationally inelastic DCS (table 2). We have shown these data in figure 20 for the S^0 and S^1 cases by using rotational transitions only up to the $|J-J'|=6$ value. We see that the two quantities S^0 and S^1 are exactly equal to each other; this is consistent with the observation of Shimamura (1981) that the energy-loss cross sections are independent of the initial rotational state of the molecule. It proves the fact that we do not need more rotational states (higher than $\Delta J = 6$) in our calculation in order to prove the sum rule discussed by Shimamura (1983). Figure 21 displays the differential energy-loss (equation (14)) cross section at a few selected energies. Note that the energy-loss cross sections increase with an increase in energy. In general,

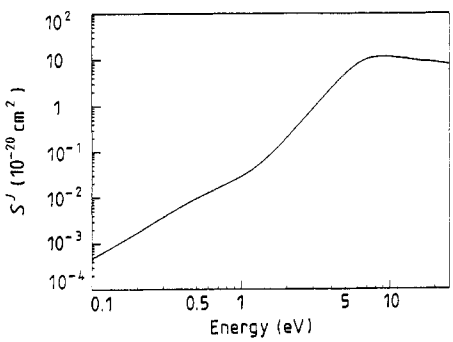

Figure 20. Stopping cross sections, S^0 and S^1, for e-CH_4 collisions as a function of impact energy. Note that S_0 and S_1 coincide and are both represented by the curve.

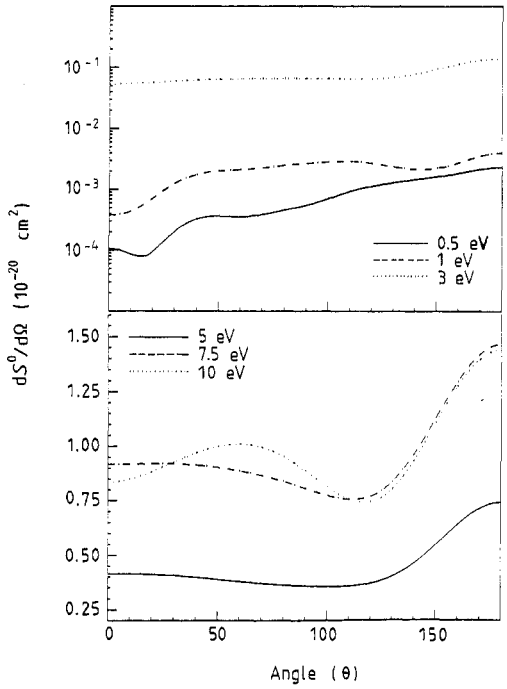

Figure 21. Energy-loss cross sections (equation (14)) at 0.5, 1, 3, 5, 7.5 and 10 eV for the 3-CH_4 collisions as a function of scattering angle.

these cross sections are very small as expected due to the strong elastic $0 \rightarrow 0$ channel. Since the $0 \rightarrow 4$ cross section exhibits the 7–8 eV structure and is stronger than the $0 \rightarrow 3$ excitation, the S^J stopping cross section is characterised by this broad feature around 7–10 eV (figure 20). There is a tendency of the energy-loss cross sections (figure 21) to increase towards higher angles.

4. Conclusions

We conclude that low-energy e-CH_4 rotationally elastic and inelastic scattering can be described realistically if exact exchange treatment is supplemented by a polarisation potential used in this paper. This polarisation potential is parameter free and easy to calculate. It is based on a *non-penetrating* approximation introduced by Temkin (1957) in which the perturbation of the molecule is neglected when the incident electron is *inside* the molecular charge cloud. There is much work to be done to produce an *ab initio* polarisation potential but the present approximate approach is proving very successful. We are presently testing this approach on other small polyatomic molecules.

We note that Brescansin *et al* (1989) and Rescigno *et al* (1989) tackle the problem of polarisation interaction via a basis set method. It will be interesting to see if this approach gives accurate results for very low electron energies (below 3 eV) and also at small angles at all energies; this is apparent so far in the Brescansin *et al* (1989) results. Our model is certainly practical and capable of producing accurate data in the region around the RT minimum ($E < 1$ eV) and our scattering length of -2.9 au is only 15% from the observed value. There are significant discrepancies between the

present and the SMP results of Brescansin *et al* (1989); nevertheless, there is an over all qualitative agreement between these two models.

Acknowledgment

This research was partially supported by the SERC grant no GR/E/94388. One of us (AJ) gratefully acknowledges the support by the FSU Supercomputer Research Institute (SCRI) which is partially funded by the US Department of Energy through contract no DE-FC05-85ER250000. AJ extends his thanks to the Queen's University of Belfast for inviting him during the summer of 1989 where a part of this work was finished. This research was also partially funded by the US Army Office of Scientific Research under contract no DAAL03-89-9-0111.

References

Abusalbi N, Eades R A, Nam T, Thirumalai D, Truhlar D G and Dupuis M 1983 *J. Chem. Phys.* **78** 1213
Abusalbi N, Schwenke D W, Mead C A and Truhlar D G 1987 *Theor. Chim. Acta* **71** 259
Bloor J E and Sherrod R F 1986 *J. Phys. Chem.* **90** 5508
Bose T K, Sochanski J S and Cole R H 1972 *J. Chem. Phys.* **57** 3592
Brescansin L M, Lima M A P and McKoy V 1989 *Phys. Rev.* A **40** 5577
Curry P J, Newell W R and Smith A C H 1985 *J. Phys. B: At. Mol. Phys.* **18** 2303
Chase D M 1956 *Phys. Rev.* **104** 838
Dababneh M S, Hsieh Y F, Kauppila W E, Kwan C K, Smith S J, Stein T S and Uddin M N 1988 *Phys. Rev.* A **38** 1207
Ferch J, Granitz B and Raith W 1985 *J. Phys. B: At. Mol. Phys.* **18** L445
Gianturco F A and Jain A 1986 *Phys. Rep.* **143** 348
Gianturco F A, Jain A and Pantano L C 1987 *J. Phys. B: At. Mol. Phys.* **20** 571
Gianturco F A and Scialla S 1987 *J. Phys. B: At. Mol. Phys.* **20** 3171
Gianturco F A and Thompson D G 1976a *Chem. Phys.* **14** 111
—— 1976b *J. Phys. B: At. Mol. Phys.* **9** L383
—— 1980 *J. Phys. B: At. Mol. Phys.* **13** 613
Haddad G N 1985 *Aust. J. Phys.* **38** 677
Hara S 1967 *J. Phys. Soc. Japan* **22** 710
Jain A 1983 *J. Chem. Phys.* **78** 6579
—— 1986a *Phys. Rev.* A **34** 954
—— 1986b *Phys. Rev.* A **34** 3707
Jain A and Thompson D G 1982 *J. Phys. B: At. Mol. Phys.* **15** L631
—— 1983 *J. Phys. B: At. Mol. Phys.* **16** 3077
Jain A, Weatherford C A, McNaughten P and Thompson D G 1989 *Phys. Rev.* A **40** 6730
Jain A and Thompson D G 1990 to be published
Jones R K 1985 *J. Chem. Phys.* **82** 5424
Lane N F 1980 *Rev. Mod. Phys.* **40** 29
Lima M A P, Gibson T L, Huo W M and McKoy V 1985 *Phys. Rev.* A **32** 2696
Lima M A P, Watari K and McKoy V 1989 *Phys. Rev.* A **39** 4312
Lohmann B and Buckman S J 1986 *J. Phys. B: At. Mol. Phys.* **19** 2565
McNaughten P and Thompson D G 1988 *J. Phys. B: At. Mol. Opt. Phys.* **21** L703
Müller R, Jung K, Kochem K H, Sohn W and Ehrhardt H 1985 *J. Phys. B: At. Mol. Phys.* **18** 3971
Norcross D W 1982 *Phys. Rev.* A **25** 764
O'Connel J K and Lane N F 1983 *Phys. Rev.* A **27** 1893
Ohmori Y, Kitamori K, Shimozuma M and Tagashira H 1986 *J. Phys. D: Appl. Phys.* **19** 437
Pople J A and Schofield P 1957 *Phil. Mag.* **2** 591
Rescigno T N, McCurdy C W and Schneider B I 1989 *Phys. Rev. Lett.* **63** 248
Rohr K 1980 *J. Phys. B: At. Mol. Phys.* **13** 4897

Salvini S S and Thompson D G 1981 *J. Phys. B: At. Mol. Opt. Phys.* **14** 3797
Shimamura I 1981 *Phys. Rev.* A **23** 3350
—— 1983 *Phys. Rev.* A **28** 1357
Shyn T W and Cravens T E 1989 *J. Phys. B: At. Mol. Opt. Phys.* to be published
Sohn W, Jung K and Ehrhardt M 1983 *J. Phys. B: At. Mol. Phys.* **16** 891
Sohn W, Kochem K H, Scheuerlein K M, Jung K and Ehrhardt H 1986 *J. Phys. B: At. Mol. Phys.* **19** 3625
Tanaka H 1979 *Symp. on Electron-Molecule Collisions* ed I Shimamura and M Matsuzawa (Tokyo: University of Tokyo Press) p 31
Tanaka H, Okada T, Boesten L, Suzuki T, Yamamoto T and Kubo M 1982 *J. Phys. B: At. Mol. Phys.* **15** 3305
Temkin A 1957 *Phys. Rev.* **107** 1004
Yuan J 1988 *J. Phys. B: At. Mol. Opt. Phys.* **21** 3113